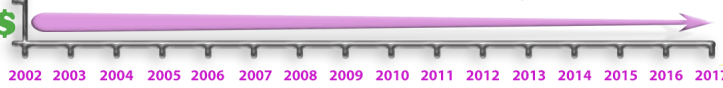




15 Years: Top Quality, No Price Increases



## Extracellular Isoforms of CD6 Generated by Alternative Splicing Regulate Targeting of CD6 to the Immunological Synapse

This information is current as of July 26, 2017.

Mónica A. A. Castro, Marta I. Oliveira, Raquel J. Nunes, Stéphanie Fabre, Rita Barbosa, António Peixoto, Marion H. Brown, Jane R. Parnes, Georges Bismuth, Alexandra Moreira, Benedita Rocha and Alexandre M. Carmo

*J Immunol* 2007; 178:4351-4361; ;  
doi: 10.4049/jimmunol.178.7.4351  
<http://www.jimmunol.org/content/178/7/4351>

- 
- References** This article **cites 53 articles**, 28 of which you can access for free at:  
<http://www.jimmunol.org/content/178/7/4351.full#ref-list-1>
- Subscription** Information about subscribing to *The Journal of Immunology* is online at:  
<http://jimmunol.org/subscription>
- Permissions** Submit copyright permission requests at:  
<http://www.aai.org/About/Publications/JI/copyright.html>
- Email Alerts** Receive free email-alerts when new articles cite this article. Sign up at:  
<http://jimmunol.org/alerts>



# Extracellular Isoforms of CD6 Generated by Alternative Splicing Regulate Targeting of CD6 to the Immunological Synapse<sup>1</sup>

Mónica A. A. Castro,<sup>2\*</sup> Marta I. Oliveira,<sup>2\*†</sup> Raquel J. Nunes,<sup>\*†</sup> Stéphanie Fabre,<sup>‡</sup> Rita Barbosa,<sup>\*</sup> António Peixoto,<sup>§</sup> Marion H. Brown,<sup>¶</sup> Jane R. Parnes,<sup>||</sup> Georges Bismuth,<sup>‡</sup> Alexandra Moreira,<sup>\*</sup> Benedita Rocha,<sup>§</sup> and Alexandre M. Carmo<sup>3\*†</sup>

The great majority of mammalian genes yield multiple transcripts arising from differential mRNA processing, but in very few instances have alternative forms been assigned distinct functional properties. We have cloned and characterized a new isoform of the accessory molecule CD6 that lacks the CD166 binding domain and is expressed in rat and human primary cells. The novel isoform, CD6Δd3, results from exon 5 skipping and consequently lacks the third scavenger receptor cysteine-rich (SRCR) domain of CD6. Differential expression of the SRCR domain 3 resulted in a remarkable functional difference: whereas full-length CD6 targeted to the immunological synapse, CD6Δd3 was unable to localize at the T cell:APC interface during Ag presentation. Analysis of expression of CD6 variants showed that, while being more frequent in coexpression with full-length CD6, the CD6Δd3 isoform constituted the sole species in a small percentage of T cells. In the rat thymus, CD6Δd3 is less represented in double-positive thymocytes but is detectable in nearly 50% of single-positive CD4 or CD8 thymocytes, suggesting that CD6 switching between full-length and Δd3 isoforms may be involved in thymic selection. Strikingly, CD6Δd3 is markedly up-regulated upon activation of T lymphocytes, partially substituting full-length CD6, as evaluated by RT-PCR analysis at the single-cell level, by immunoblotting, and by flow cytometry using Abs recognizing SRCR domains 1 and 3 of human CD6. This elegant mechanism controlling the expression of the CD166 binding domain may help regulate signaling delivered by CD6, through different types of extracellular engagement. *The Journal of Immunology*, 2007, 178: 4351–4361.

The TCR recognition of peptide-MHC complexes expressed on APCs involves the formation of a tight cell-cell contact area, the immunological synapse (IS),<sup>4</sup> where individual proteins are selectively partitioned (1, 2). The model of

synapse formation predicts an initial stabilization of the contact by engaged integrins, which anchor the region of the contact and allow the TCRs to scan MHC-peptide complexes (3). With time, stably engaged TCR complexes coalesce into a central area (cSMAC; central supramolecular activation clusters), surrounded by a ring (pSMAC; peripheral supramolecular activation clusters) enriched in the integrin LFA-1 (2, 4). In the mature synapse, cSMAC are also enriched in the costimulatory molecule CD28 and the CD4 or CD8 coreceptors (3, 5). It has been suggested that the formation of the synapse is favored by receptor-ligand interactions of small auxiliary molecules such as CD2-CD58 and CD28-CD80 that stabilize the cell contact by the formation of low-affinity interactions, in a size dependent-manner. According to this model, the small adhesion pairs cluster at a tight membrane region, thus segregating larger glycoproteins such as CD43 or CD45 (1, 6).

CD6 is a 100- to 130-kDa surface glycoprotein expressed primarily on medullary thymocytes and mature T lymphocytes (7). CD6 has been regarded as a costimulatory molecule as Ab-mediated CD6 cross-linking can potentiate proliferative T cell responses (8–10). Moreover, a subpopulation of CD6-negative T cells displayed lower alloreactivity in MLRs compared with normal CD6<sup>+</sup> T cell populations (11). CD6 could additionally play a role in thymocyte maturation, because CD6 Abs have been shown to partially block the adhesion of thymocytes to thymic epithelial cells (12). This observation also provided the first evidence that CD6 had a cell surface ligand. A requirement for ligand engagement for costimulatory effects of CD6 was shown by inhibition of Ag-specific and CD3 mAb-induced T cell responses by soluble CD6 (13, 14). Recently, CD6 has been reported to accumulate at the IS, mediating early and late T cell-APC interactions required for IS maturation and cell proliferation (13, 15).

Upon CD3 engagement CD6 becomes phosphorylated on tyrosine residues, suggesting that interactions with Src homology (SH)2 domain-containing intracellular effectors may occur (16).

\*Group of Cell Activation and Gene Expression, Instituto de Biologia Molecular e Celular, Universidade do Porto, Porto, Portugal; †Instituto de Ciências Biomédicas de Abel Salazar, Universidade do Porto, Porto, Portugal; ‡Institut National de la Santé et de la Recherche Médicale Unité 567, Département de Biologie Cellulaire, Institut Cochin, Paris, France; §Institut National de la Santé et de la Recherche Médicale Unité 345, Institut Necker, Paris, France; ¶Sir William Dunn School of Pathology, University of Oxford, Oxford, United Kingdom; and ||Department of Medicine, Division of Immunology and Rheumatology, Stanford University School of Medicine, Stanford, CA 94305

Received for publication February 22, 2006. Accepted for publication January 10, 2007.

The costs of publication of this article were defrayed in part by the payment of page charges. This article must therefore be hereby marked *advertisement* in accordance with 18 U.S.C. Section 1734 solely to indicate this fact.

<sup>1</sup> This work was supported by Programa Operacional Ciência, Tecnologia, Inovação (POCTI), and Programa Operacional Ciência e Inovação 2010 (POCI), cofunded by the European Regional Development Fund (FEDER). M.A.A.C. is supported by a postdoctoral fellowship from Fundação para a Ciência e a Tecnologia (FCT)-Programa Operacional Sociedade da Informação; M.I.O. and R.J.N. are recipients of studentships from FCT-POCTI; S.F. is supported by the Ministère de l'Éducation Nationale et de La Recherche; J.R.P. was supported by Grant CA68675 from the National Institutes of Health; and A.P. was funded by FCT, Ligue Contre le Cancer, and Association pour la Recherche sur le Cancer. Additional support was obtained from Programa Pessoa, a Gabinete de Relações Internacionais da Ciência e do Ensino Superior (Portugal)/Egide (France) cooperation.

<sup>2</sup> M.A.A.C. and M.I.O. contributed equally to this work.

<sup>3</sup> Address correspondence and reprint requests to Dr. Alexandre M. Carmo, Institute for Molecular and Cellular Biology, Rua do Campo Alegre, Porto, Portugal. E-mail address: acarmo@ibmc.up.pt

<sup>4</sup> Abbreviations used in this paper: IS, immunological synapse; cSMAC, central supramolecular activation cluster; pSMAC, peripheral supramolecular activation cluster; SH, Src homology; SRCR, scavenger receptor cysteine rich; YFP, yellow fluorescent protein; SEA, staphylococcal enterotoxin A; DP, double positive; SP, single positive.

Copyright © 2007 by The American Association of Immunologists, Inc. 0022-1767/07/\$2.00

An interaction with the SH2 domain of SLP-76 has been shown to be critical for the costimulatory effects of CD6 (17). The cytoplasmic domain of CD6 is unusually long and also contains two well-conserved proline-rich sequences, which are potential binding sites for SH3 domain-containing proteins well suited for signal transduction (16, 18). Indeed, the rat homolog of CD6 has been shown to associate with protein tyrosine kinases of different families, namely Src-family kinases Lck and Fyn, Zap70 of the Syk family, and the Tec-family kinase Itk (19). CD6 has additionally been shown to associate at the surface of T cells with CD3 (13) and with the structurally related receptor CD5 (19, 20). However, there are still no data proposing a functional role for these interactions.

By contrast, the molecular basis of the interaction between CD6 and the extracellular physiological ligand, CD166, has been comprehensively investigated in human and murine models (21). CD166 is a widely expressed glycoprotein containing five Ig superfamily domains, of which the N-terminal domain has been shown to bind to the third scavenger receptor cysteine-rich (SRCR)-type domain of CD6, the membrane-proximal domain (22, 23). The residues of CD6 involved in the contact with CD166 are located in the E-F loop, a region that, in the particular case of the third domain of CD6, is most divergent from all known SRCR domains (24). The resulting interaction between CD6 and CD166 is therefore unusual, because most other T cell surface proteins mediating cell-cell interactions bind through their N-terminal domains. However, affinity and kinetic measurements revealed that, in solution, binding occurs with a  $K_d$  of 0.4–1.0  $\mu\text{M}$  (14), relatively strong compared with most other leukocyte adhesion pairs, albeit in the range of low-affinity interactions characteristic of cell surface receptors (25–27).

The human, rat, and mouse *Cd6* genes contain 13 exons, of which the last 6 code for the cytoplasmic tail. Numerous CD6 isoforms have been reported that result from alternative splicing of the exons coding for the cytoplasmic domain (18, 28–30), but no specific physiological function has been attributed to any of these isoforms. Exon 7 contains the sequence coding for the transmembrane domain, and the first 6 exons code for most of the extracellular domain. Alignment of the CD6 extracellular sequence with that of the scavenger receptor domain of Mac-2 binding protein, for which a crystal structure has been obtained (24), predicts that each scavenger-type domain of CD6 is encoded by a single exon, and that removal of each of these exons would result in a protein only devoid of the correspondent domain. We have obtained from rat thymocytes and peripheral rat and human T cells, cDNAs of CD6 omitting exon 5, whose corresponding translated polypeptides lack the SRCR domain 3. This CD6 isoform, CD6 $\Delta$ d3, is present in all T lineage cells studied and is up-regulated upon activation, paralleling a decline in the expression of full-length CD6. The failure of CD6 $\Delta$ d3 binding to CD166 highlights the role of domain 3 in addressing CD6 to the IS, and the down-modulation of domain 3 induced upon T cell activation reveals a rare mode of positional control of cell surface receptors dependent on alternative mRNA splicing.

## Materials and Methods

### Cells and cell lines

Rat thymocytes, splenocytes, and cervical lymph node cells were from 9- to 12-wk-old Lewis male rats (Charles River Laboratories). Human primary T cells were isolated from peripheral blood by centrifugation on a Ficoll gradient followed by negative depletion on magnetic beads (T cell-negative isolation kit; Dynal Biotech), or using the RosetteSep human T cell enrichment mixture (StemCell Technologies), where indicated. Cell lines COS7 (31) and Raji (32) were maintained in RPMI 1640 supple-

mented with 10% FCS, 1 mM sodium pyruvate, 2 mM L-glutamine, penicillin G (50 U/ml), and streptomycin (50  $\mu\text{g}/\text{ml}$ ).

### Abs and reagents

Rat mAbs used were CD6-OX52 (33) (a gift from N. Barclay, University of Oxford, U.K.), TCR-R73 (34), and CD28-JJ319 (35) (gifts from T. Hünig, University of Würzburg, Germany). Conjugated mAbs used for cell sorting were as follows: biotinylated CD4-W3/25 (obtained from Serotec); CD6-OX52 FITC-labeled, CD3-1F4, and CD45RC-OX22, conjugated with PE, biotinylated CD8 $\beta$ -341 and CD134-OX40, and CD4-OX35 conjugated with allophycocyanin (obtained from BD Biosciences). Biotinylated Abs were detected with streptavidin conjugated with PE, PE-Cy7, or allophycocyanin. Human mAbs were as follows: OX126 (17), specific for human CD6 domain 3, FITC-labeled UMCD6 (9), anti-domain 1 of CD6 (obtained from Ancell); MEM-98 (36) (anti-CD6 domain 1; a gift from V. Hořejší, Academy of Sciences, Prague, Czech Republic), CD166-3A6 (37) (BD Pharmingen); and CD71 (DakoCytomation). Goat anti-mouse peroxidase conjugated was obtained from Molecular Probes Europe and rabbit anti-mouse FITC-labeled from DakoCytomation. Biotinylated proteins were detected in Western blotting with ExtrAvidin peroxidase (Sigma-Aldrich).

### cDNA cloning and plasmids

Rat CD6 cDNAs were cloned as described previously (19). Full-length rat CD6 (CD6FL) cDNA (19) was extracted from pCR2.1-TOPO vector (Invitrogen Life Technologies) using *Spe*I and *Apa*I and blunt-end cloned into the expression vector pEF-BOS (38). rCD6 $\Delta$ d3/pEF-BOS was obtained by digestion with *Sma*I of a sequence flanking the alternatively spliced exon 5 from the rCD6 $\Delta$ d3/pCR2.1-TOPO template. The vector encoding rat CD6FL-YFP was produced as follows: rat CD6 cDNA was amplified from the original clone rCD6/pCR2.1-TOPO (19) by PCR using as the reverse primer 5'-GCAGAATTCGAAGCTTGGCTGCTCCAATGTCATCG-3'. The PCR product was then cloned into the pEYFP-N1 vector (Clontech Laboratories) in frame with the N-terminal sequence of the yellow fluorescent protein (YFP), in the *Hind*III restriction sites included in the primers. The rCD6 $\Delta$ d3/pEYFP-N1 construct was obtained by digestion as described above and cloned in frame with pEYFP-N1. A cytoplasmic deletion mutant of rat CD6 fused to YFP was produced by PCR from rCD6/pCR2.1-TOPO using as reverse primer 5'-CTACTAAAGCTTTTGTCTTTGGC TTTCAAGAG-3', terminating just after the codon of the fifth amino acid of the cytoplasmic domain. The PCR product was cloned into the *Hind*III restriction site of the pEYFP-N1 vector to produce rCD6CY5/pEYFP-N1.

Total RNA was isolated from human PBMC and E6.1 Jurkat cells using the RNA extraction kit (Qiagen). cDNA was obtained using the ThermoScript RT-PCR system (Invitrogen Life Technologies) from total RNA primed with oligo(dT). Human *Cd6* was amplified with primer design based on the reported sequence (GenBank accession no. U34625). The following primers were used in the cloning of the isoforms: forward primer spanning the initiation codon (shown in bold) 5'-CGCGGATCCTCTAGATGTGGCTCTTCTTC GGGATCACTGGATTG-3' and reverse primer in the exon 7 (TM-coding sequence) of human *Cd6* 5'-GGAGCATTAGCTCCCGAGATTCCTTG-3'. The PCR fragments were cloned into pCR2.1-TOPO vector. The sequences were confirmed by dedeoxy sequencing.

Human CD6FL/pEGFP-N1 was produced by amplifying a full-length sequence from the clone CD6/pBJ-neo (18) by PCR, using as the forward primer 5'-CGCGGATCCTCTAGATGTGGCTCTTCTTCGGGATCACTGGATTG-3' and the reverse primer 5'-CTACTAGAATCCGCTGCGCTGATGTC ATCG-3'. The PCR product was then cloned into the *Bam*HI restriction site of the pEGFP-N1 vector (Clontech Laboratories) producing CD6FL/pEGFP-N1. The isoform CD6 $\Delta$ d3 was amplified from the vector pCR2.1-TOPO using the primer M13-R from the vector as the forward primer, and a reverse primer in the exon 7 of human CD6 including a naturally occurring *Eco*RI restriction site 5'-CTACTAGAATCCAGAACGATGGAGGG GATGAGGAGCATTAGCTCCCGAGATTCCTTG-3'. The PCR product was inserted in the CD6FL/pEGFP-N1 producing CD6 $\Delta$ d3/pEGFP-N1. A cytoplasmic deletion mutant of human CD6 fused to GFP was produced by PCR from CD6/pBJ-neo with the forward primer 5'-CTCCAGACATGTG GCTCTTCTTCGG-3' and the reverse primer 5'-GCCTTCATCTCTTGA GAATTAAGGAAAA-3', terminating just before the first tyrosine residue codon of the cytoplasmic domain. The PCR product was cloned into the TOPO cloning site of pcDNA3.1/CT-GFP-TOPO, using GFP Fusion TOPO TA Expression Kits (Invitrogen Life Technologies; version I), to produce CD6CY5/pcDNA3.1/CT-GFP-TOPO.

Rat CD166 cDNA was obtained from total RNA isolated from Lewis rat lungs and reverse transcribed using a gene-specific primer 5'-CC AGGACAGCTTAGTAGGAT-3'. Amplification of the full-length molecule was performed using as forward primer 5'-TAGTAGAAGCTT



CTAGGAGGAGGAATATGGC-3' and reverse primer 5'-CTACTACTCGAGACTCCTCTCTTAGGCTTCTG-3'. Cloning the resulting PCR product into the *Hind*III-*Pst*I restriction site of the pECFP-N2 vector handled rCD166/pECFP-N2.

### Cell transfections

Rat CD6FL and CD6 $\Delta$ d3 in pEF-BOS, or the empty vector, were transiently transfected in COS7 cells following the procedures described previously (39).

Transient transfections of primary T lymphocytes ( $5 \times 10^6$  cells) were performed with 5  $\mu$ g of rat CD6FL/pEYFP-N1, CD6 $\Delta$ d3/pEYFP-N1 or CD6CY5/pEYFP-N1 or human CD6FL/pEGFP-N1, CD6 $\Delta$ d3/pEGFP-N1 or CD6CY5/pcDNA3.1/CT-GFP-TOPO plasmids using the Human T cell Nucleofector kit (Amaxa), and T cells were used 24 h posttransfection. Transfection of Raji B cells was performed as follows:  $10^7$  cells were centrifuged, resuspended in 900  $\mu$ l of prewarmed complete medium, mixed with 20  $\mu$ g of rat CD166/pECFP-N2 plasmid, and transferred into a GenePulse cuvette (Bio-Rad). Electroporation was performed in a Bio-Rad Gene Pulser II electroporator at 950  $\mu$ F and 260 V. Cells were maintained in complete medium at 37°C and used 48 h after transfection.

### Cell surface biotinylation, immunoprecipitations, and Western blotting

Cell surface biotinylation, immunoprecipitations and detection of biotinylated Ags, and immunoblotting were performed as described previously (40).

### Single-cell RT-PCR analysis

RT-PCR were performed on single cells purified on the basis of their expression of selected markers after two rounds of cell sorting using a FACSVantage equipped with an automatic deposition unit (BD Biosciences). The characteristics and sensitivity of the RT-PCR method have been previously described in detail (41). Briefly, cells were lysed and the RNA reverse transcribed using a *Cd6*-specific 3' primer, 5'-GAGTCCTTATCCTTACGCT-3', and the resulting cDNAs amplified in a two-step nested PCR. The 5' primers used were as follows: 5'-ATCCACCGTGACCAAGTGAA-3' and 5'-AGACCAGTACTGCGGTCACA-3' (nested), and the same reverse primer was used for the reverse transcription reaction. None of the primer combinations amplifies genomic DNA.

### Flow cytometry

Flow cytometry was performed as described previously (40).

### Cellular activation

A cell suspension was obtained from rat spleen, and  $2 \times 10^6$  cells/ml were activated for 72 h in vitro by incubation with anti-TCR (R73) plus anti-CD28 (JJ319) mAbs used at 2–10  $\mu$ g/ml, or left untreated. Cells were incubated at 37°C with 5% CO<sub>2</sub> and, after the indicated period, collected, labeled for OX40, sorted or lysed, and analyzed by immunoblotting.

Human primary T cells were activated by incubating  $3 \times 10^6$  cells/ml with PHA-p at 5  $\mu$ g/ml in RPMI 1640, at 37°C with 5% CO<sub>2</sub>, or left untreated. After 72 h, cells were collected and analyzed by flow cytometry or immunoblotting.

### Conjugate formation and fluorescence analysis

Raji B cells were incubated with a mix of superantigens (staphylococcal enterotoxin A (SEA), SEB, and SEC3, 200 ng/ml each; Toxin Technologies) and plated on poly-D-lysine-coated glass coverslips for 30 min at 37°C. T cells were added to APCs and then incubated at 37°C for 45 min. Cells were fixed with 4% paraformaldehyde in PBS for 10 min and washed several times with PBS before analysis. Where indicated, T cells were preincubated, for 30 min at 4°C, with the mAbs OX126 or UMCd6-FITC, and Raji B cells preincubated with 3A6 (CD166), all at 10  $\mu$ g/ml, or left untreated. Immunofluorescence and transmission light images were acquired on an Eclipse TE300 inverted microscope (Nikon) equipped with a cooled CCD camera (CoolSNAPFx; Roper Scientific). Images were acquired and analyzed using the Metamorph software (Roper Scientific). Conjugate formation and synapse localization of CD6 or CD166 were quantified with blind scoring, counting a minimum of 50 productive conjugates in each of two or more experiments, and each experiment was observed by two to three examiners.

## Results

### A novel isoform of rat CD6 devoid of the CD166 binding domain arises from alternative splicing

Human and mouse CD6 possess several isoforms characterized by cytoplasmic tails of variable lengths, resulting from alternative splicing of exons coding for the intracellular domain (18, 28–30). Subsequent to our recent cloning of a cDNA of rat CD6 (19) containing all 13 exons homologous to the mouse and human sequences, we proceeded to a systematic search for novel rat CD6 isoforms. Using total RNA isolated from Lewis male rat spleens, cDNAs were obtained by reverse transcription followed by PCR using primers complementary to sequences immediately before and after the coding sequence. We obtained five cDNA species displaying distinct mobility on agarose gels (Fig. 1A). Sequencing confirmed the longest product as full-length CD6. Interestingly, sequencing of the third largest product (indicated by an arrow) revealed a novel isoform lacking not a cytoplasmic-coding exon, but missing instead the sequence corresponding to exon 5 (GenBank accession no. AY683561). Alignment of the corresponding amino acid sequence with that of wild-type rat CD6 shows that this cDNA codes for a novel isoform lacking the third SRCR domain, which contains the binding site for the ligand, CD166 (Fig. 1, B–D).

### CD6 $\Delta$ d3 is expressed at the cell surface

To verify whether the novel isoform, CD6 $\Delta$ d3, could be correctly folded, transported, and expressed at the cell surface, we cloned the corresponding cDNA into the expression vector pEF-BOS and used it for transfecting COS7 cells. In parallel, COS7 cells were transfected with rCD6FL/pEF-BOS, encoding full-length rat CD6, and also with an empty vector. Forty-eight hours after transfection, cells were analyzed for membrane expression of CD6 by immunoprecipitation, using the CD6-specific mAb OX52, and streptavidin-peroxidase detection from lysates of surface biotinylated cells. As shown in Fig. 2, detection of CD6 $\Delta$ d3 confirmed its correct folding and expression at the cell surface. The apparent molecular mass of this isoform is 112 kDa, compared with 126 kDa of full-length CD6. No product was detected in the lane corresponding to empty vector.

### Full-length CD6, but not CD6 $\Delta$ d3, targets to the IS upon T cell-APC conjugate formation

An accumulation of human CD6 at the IS has been recently reported in Jurkat-Raji cell conjugates (20). We thus tested the dependence on CD166-binding interactions for CD6 recruitment to the synapse, by using both CD6FL and CD6 $\Delta$ d3 isoforms. T cells were transfected with constructs coding for either CD6FL-YFP or CD6 $\Delta$ d3-YFP fusion proteins. In isolated T cells, the distribution of both isoforms is homogenous at the plasma membrane (Fig. 3A), a result which additionally confirms that CD6 $\Delta$ d3 can be efficiently expressed at the plasma membrane. Incubation of T cells with Raji B cells primed with superantigen, but not expressing rat CD166, did not change the pattern of CD6FL or CD6 $\Delta$ d3 distribution at the cell surface (Fig. 3B). However, when Ag-primed Raji expressed rat CD166 (shown in green) and T cells expressed CD6FL, both molecules were able to concentrate at the Raji-T cell contact zone (Fig. 3C, left panels, and E). Interestingly, the CD6 $\Delta$ d3 isoform did not efficiently relocalize to the synapse, and, moreover, did not induce colocalization of CD166 as well (Fig. 3C, right panels, and E). This result indisputably proves that the effective CD166-dependent CD6 recruitment to the synapse relies on the presence of the third SRCR domain of CD6. Conversely, rat CD166 targets to the synapse when its T cell ligand rat CD6, expressing the SRCR domain 3, is expressed at the T cell surface.

To verify whether intracellular interactions with other signaling intermediates or with the cytoskeleton could also be involved in the

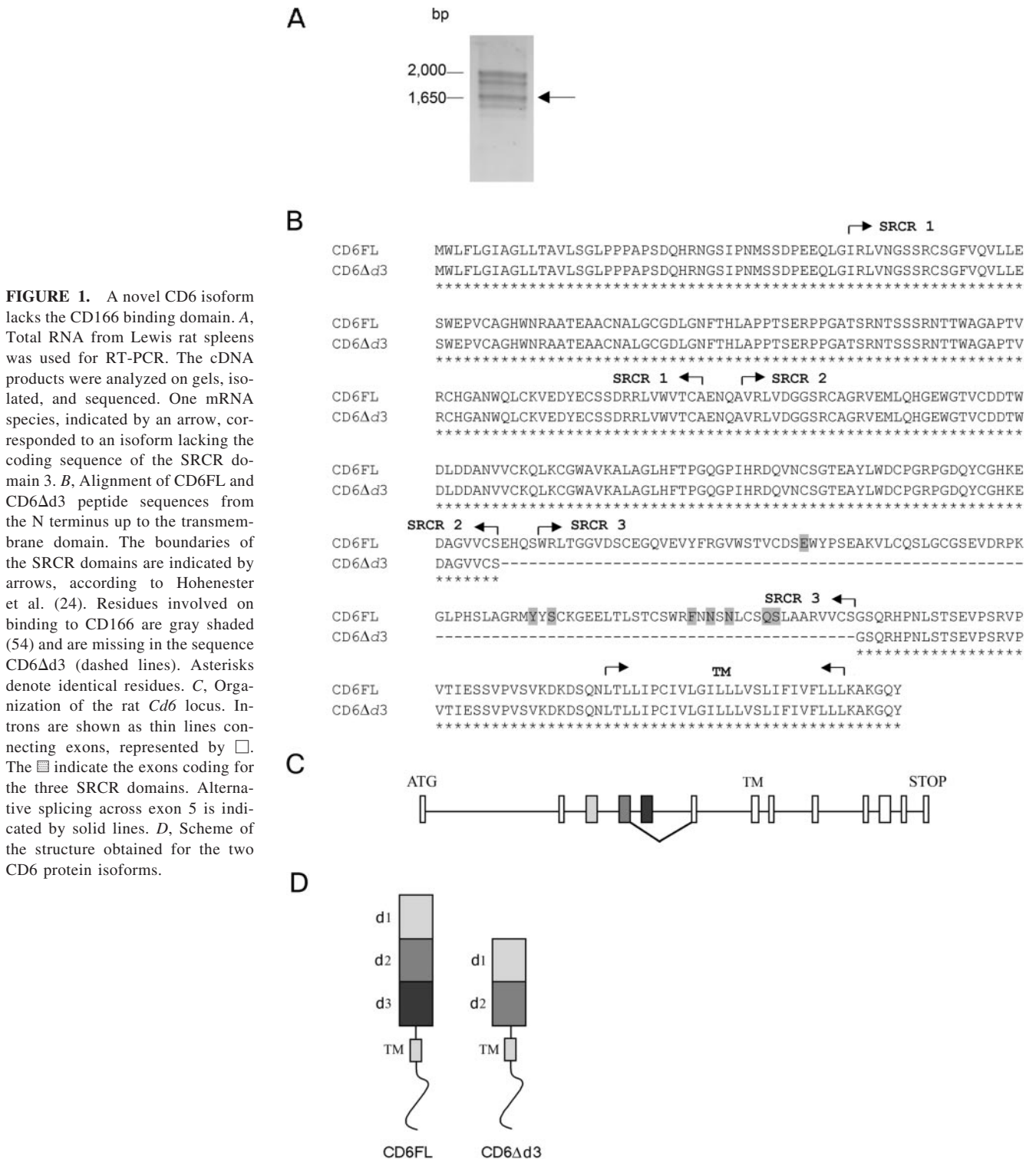


**FIGURE 1.** A novel CD6 isoform lacks the CD166 binding domain. *A*, Total RNA from Lewis rat spleens was used for RT-PCR. The cDNA products were analyzed on gels, isolated, and sequenced. One mRNA species, indicated by an arrow, corresponded to an isoform lacking the coding sequence of the SRCR domain 3. *B*, Alignment of CD6FL and CD6Δd3 peptide sequences from the N terminus up to the transmembrane domain. The boundaries of the SRCR domains are indicated by arrows, according to Hohenester et al. (24). Residues involved on binding to CD166 are gray shaded (54) and are missing in the sequence CD6Δd3 (dashed lines). Asterisks denote identical residues. *C*, Organization of the rat *Cd6* locus. Introns are shown as thin lines connecting exons, represented by □. The ■ indicate the exons coding for the three SRCR domains. Alternative splicing across exon 5 is indicated by solid lines. *D*, Scheme of the structure obtained for the two CD6 protein isoforms.

translocation of CD6 to the IS, T cells were induced to express CD6CY5, a truncated form of the protein retaining only 5 aas of the cytoplasmic domain, fused to YFP. These cells were incubated with Ag-primed Raji cells, expressing rat CD166 (Fig. 3D). The truncated form of CD6 was found to localize in the IS as efficiently as the full-length form (Fig. 3, D and E), excluding an exclusive role for cytoplasmic domain interactions on CD6 targeting to the contact zone.

#### *Cd6* expression in different lymphoid tissues and individual cells

Given a potential distinct role of the two isoforms, we conducted a detailed analysis on the profiling of expression of *Cd6* in different

lymphoid organs, specifically addressing the frequency of *Cd6Δd3*. We performed PCR from mRNA from thymus, spleen, and lymph nodes amplifying only the sequences corresponding to the extracellular and transmembrane domains, thus excluding cytoplasmic domain isoforms. Two major isoforms were obtained in all three organs, and at similar proportions (Fig. 4A). The heaviest and most abundant product matched the entire sequence, whereas the smallest product, 300 nt shorter, matched the isoform lacking exon 5. This experiment was reproducible and PCR products from several trials were extensively sequenced and confirmed the

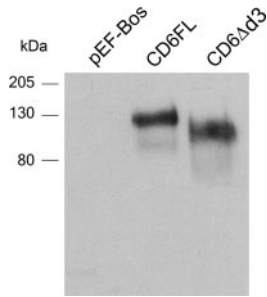


**FIGURE 2.** CD6 $\Delta$ d3 is expressed at the surface of COS7 cells. CD6FL and CD6 $\Delta$ d3 coding cDNAs were cloned in pEF-BOS and transfected in COS7 cells. Forty-eight hours posttransfection, cells were surface biotinylated, lysed, and CD6 was immunoprecipitated using OX52. Cells transfected with the empty vector were used as a negative control. Both isoforms were efficiently expressed at the cell surface.

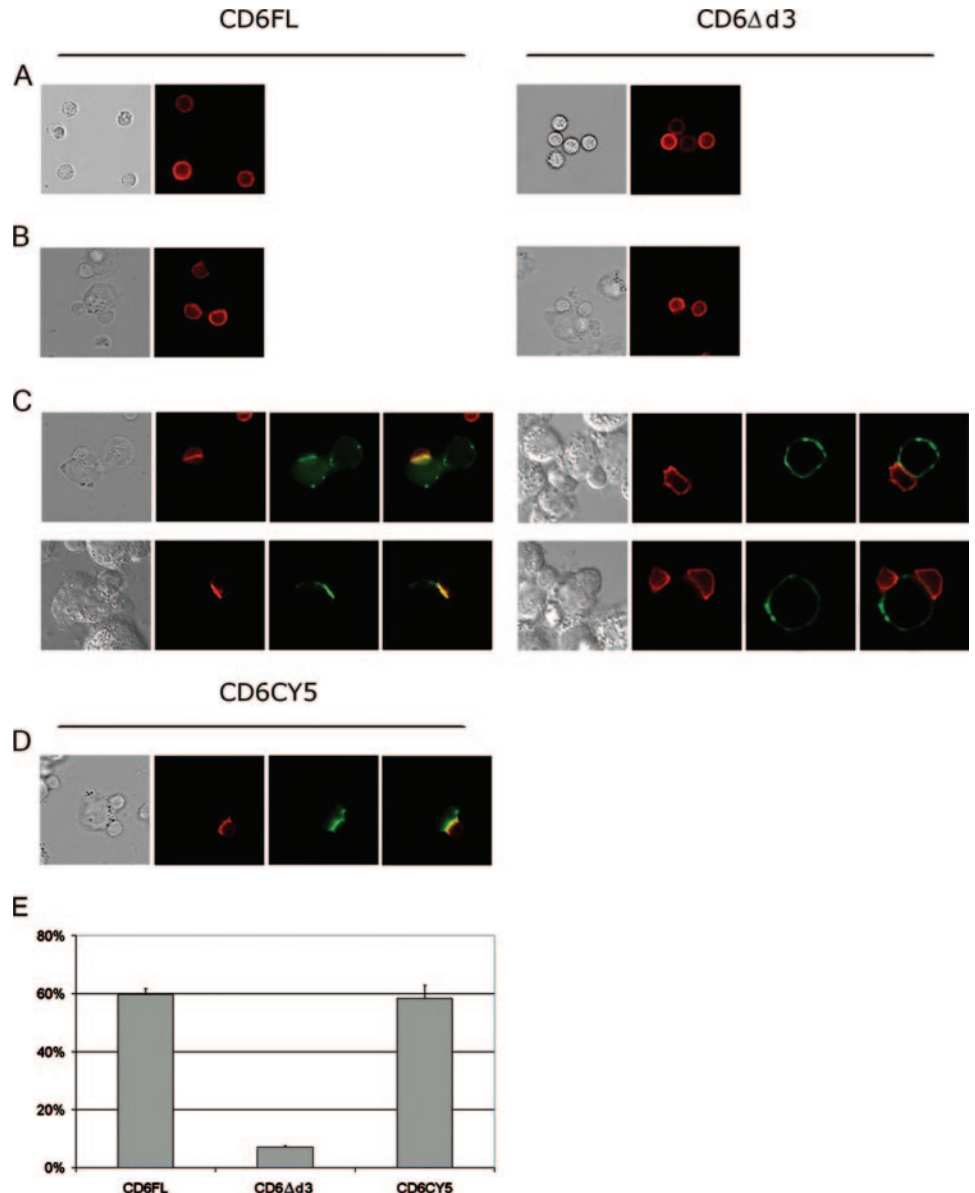
expression of only these two isoforms but not of others, for example excluding exons 3 or 4.

The pattern of expression of the CD6 gene in bulk cellular preparations suggested that both isoforms could be found in all tissues

analyzed. However, it did not clarify whether each isoform was the sole species in a given cell, or whether both isoforms could be coexpressed in the same cell. We sorted different cell populations and addressed *Cd6* expression at the single-cell level. The target populations for this study were developing thymocytes at different maturation stages as well as diverse subsets of T lymphocytes (Fig. 4B). Cells were sorted based on the protein expression of specific markers, and expression of each isoform was assayed by single-cell RT-PCR. All sorted populations were gated on CD6<sup>high</sup>-expressing cells, and thus *Cd6* amplification directly attested for plating efficiency, with no need for parallel amplification of an internal control.

PCR amplification was performed using primers flanking the spliced exon, rendering products of 452 bp for full-length *Cd6* and 148 bp for *Cd6* $\Delta$ d3. Fig. 4C shows an analysis of PCR products obtained from CD3<sup>+</sup>CD4<sup>+</sup>CD8<sup>-</sup> individual thymocytes. All possible CD6 phenotypes were present in this population, with many cells expressing only full-length CD6, a few expressing exclusively the  $\Delta$ d3 isoform, whereas others coexpressed both. In mature T cells, the frequency of *Cd6* $\Delta$ d3 expression was remarkably consistent, regardless of the cell type studied. Nearly 40% of total CD4 or CD8 T cells expressed *Cd6* $\Delta$ d3 at detectable levels (Fig. 4D, left panel). In

**FIGURE 3.** Localization of CD6 to the IS is dependent on the SRCR domain 3 of CD6 and its interaction with CD166, but not on intracellular interactions. A, Differential interferential contrast and fluorescence images of unstimulated primary T cells transfected with CD6FL-YFP (left panels) or CD6 $\Delta$ d3-YFP (right panels). Labeled CD6 is shown in red. B, IS formed between superantigen-pulsed Raji B cells and CD6FL-YFP or CD6 $\Delta$ d3-YFP-transfected primary T cells. Cells were fixed after 45 min of interaction. C, Raji B cells were transfected with CD166-CFP (detected as green) and pulsed with 1  $\mu$ g/ml superantigen mix before incubation with transfected T cells. Localization of CD6FL-YFP or CD6 $\Delta$ d3-YFP and CD166-CFP as well as fluorescence overlays are shown. Two examples of each experiment are represented. D, Interaction of T cells expressing CD6CY5-YFP with CD166-CFP expressing Raji show colocalization of CD6 and CD166. E, Frequency of cells translocating rat isoforms CD6FL, CD6 $\Delta$ d3, and CD6CY5 to the IS in T cells forming conjugates with rat CD166-expressing Raji. Positive translocation was only considered in conjugates with synaptic CD6 accumulation coinciding with a clear CD166 patch in Raji. Results are from three independent experiments, with a minimum of 50 productive conjugates considered per experiment. All counts were performed with blind scoring.





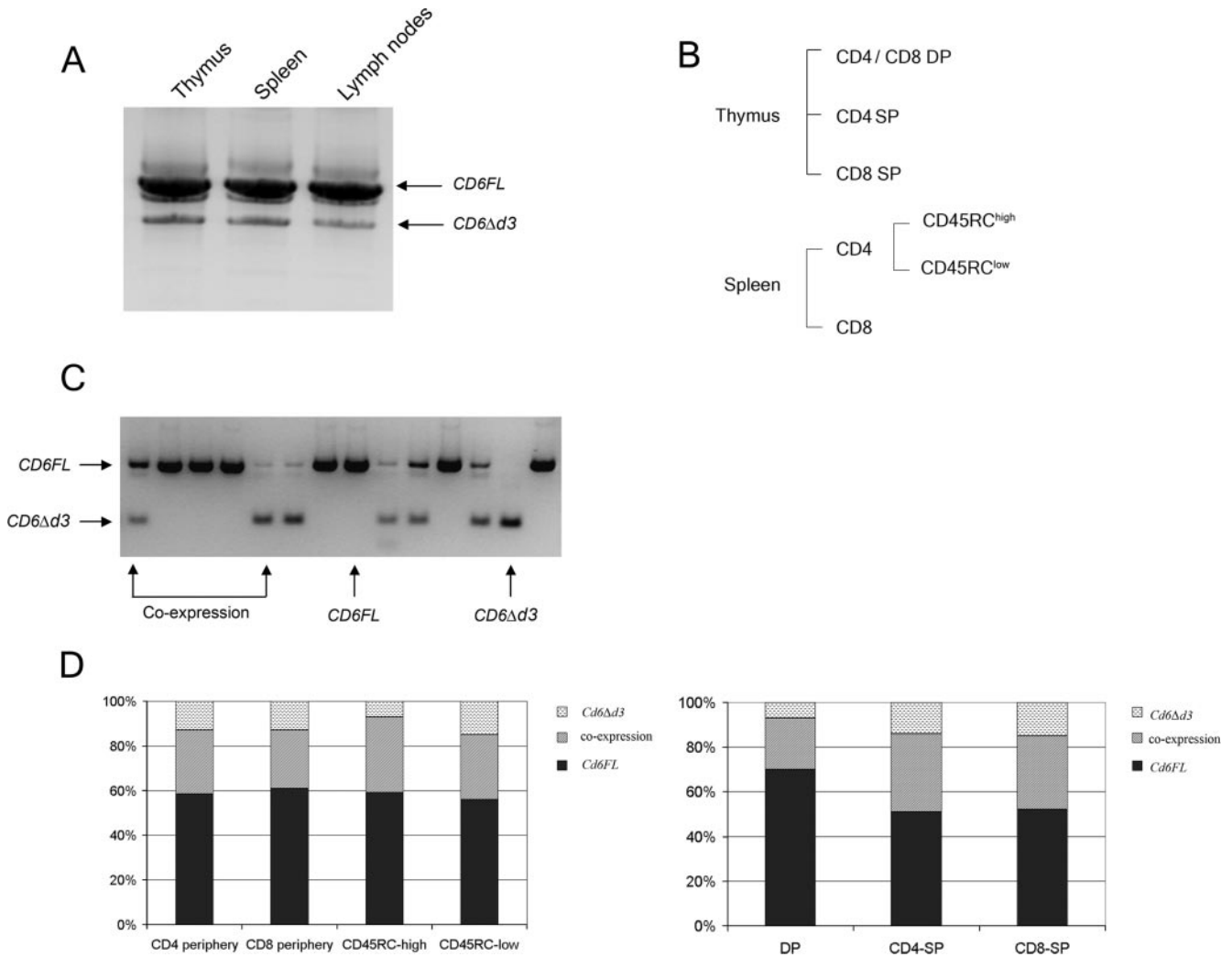


**FIGURE 4.** Expression of *Cd6* mRNA isoforms. *A*, RT-PCR analysis of the expression of *Cd6* mRNA in lymphoid organs. Total RNA was isolated from thymocytes, lymph nodes, and splenocytes, and reverse transcribed. PCR was performed amplifying the sequence between exons 1 and 7. Expression of *Cd6FL* (upper band) and *Cd6Δd3* (lower band) was detected in all lymphoid tissues. *B*, Individual cells from the population indicated were sorted: CD4/CD8 DP, CD4 SP, and CD8 SP thymocytes; and CD4 and CD8 mature T cells from spleen. CD4 T cells were further separated into CD45RC<sup>high</sup> and CD45RC<sup>low</sup> subpopulations, associated with a naive and memory phenotype, respectively. *C*, Example of expression of the two different CD6 isoforms, *Cd6FL* and *Cd6Δd3*, by individual cells. Results shown are of CD4<sup>+</sup>CD8<sup>-</sup>CD3<sup>+</sup> thymocytes. Coexpression was considered in individual cells where both isoforms could be detected, as illustrated. *D*, Frequency of *Cd6* mRNA expression in sorted populations from the periphery (left panel) and thymus (right panel). Over 40 individual cells were considered for each population. All sorted populations were gated on CD6<sup>high</sup>-expressing cells.

addition, CD4<sup>+</sup>CD45RC<sup>high</sup> and CD4<sup>+</sup>CD45RC<sup>low</sup> splenocytes, which have been associated with a naive and memory phenotype, respectively, showed no significant variation in the percentage of cells expressing *Cd6Δd3* (Fig. 4*D*, left panel), although the ratio between the number of cells expressing only *Cd6Δd3* and cells where coexpression was observed was the highest overall in memory cells and the lowest in naive cells.

As distinct from mature T cells, levels of *Cd6Δd3* expression fluctuated noticeably between different thymocyte populations. *Cd6Δd3* was least abundant in double-positive (DP) thymocytes, being expressed in just 30% of the cells (Fig. 4*D*, right panel). By contrast, nearly 50% of single-positive (SP) CD4 or CD8 thymocytes expressed *Cd6Δd3*, and no differences were registered between these two subpopulations.

#### Cell activation increases rat CD6Δd3 expression

We next analyzed the pattern of expression of rat CD6 isoforms upon cell activation. Activated T cells were generated by incubating rat splenocytes with anti-TCR plus anti-CD28 mAb over 3

days. The percentage of CD4<sup>+</sup> T cells with an activated phenotype, as determined by OX40 expression (42), increased from 20 to 91% (Fig. 5*A*). CD4<sup>+</sup>OX40<sup>+</sup> cells were sorted as individual cells and compared with the nonactivated phenotype. RT-PCR analysis of individual cells revealed a clear modification in the pattern of expression of *Cd6* isoforms following activation, with an increase in the number of cells coexpressing both isoforms (Fig. 5*B*). The relative levels of CD4 T cells expressing the *Cd6Δd3* mRNA increased significantly from 42 to 86% upon stimulation (Fig. 5*C*).

Analysis of CD6 expression at the protein level was also performed by immunoblotting. Two isoforms of CD6 with molecular masses of ~130 and 122 kDa (indicated by dashed arrows) were clearly detected in resting splenocytes. These two isoforms should be products of alternative splicing, but still retain domain 3, given that the size is very close to that displayed by full-length rat CD6 in COS7 cells (126 kDa), whereas the CD6Δd3 mutant expressed in COS7 cells had a molecular mass of 112 kDa (see Fig. 2). Splenocytes were stimulated with TCR and CD28 mAb, and after 72 h cells were collected, lysed with detergent, and CD6

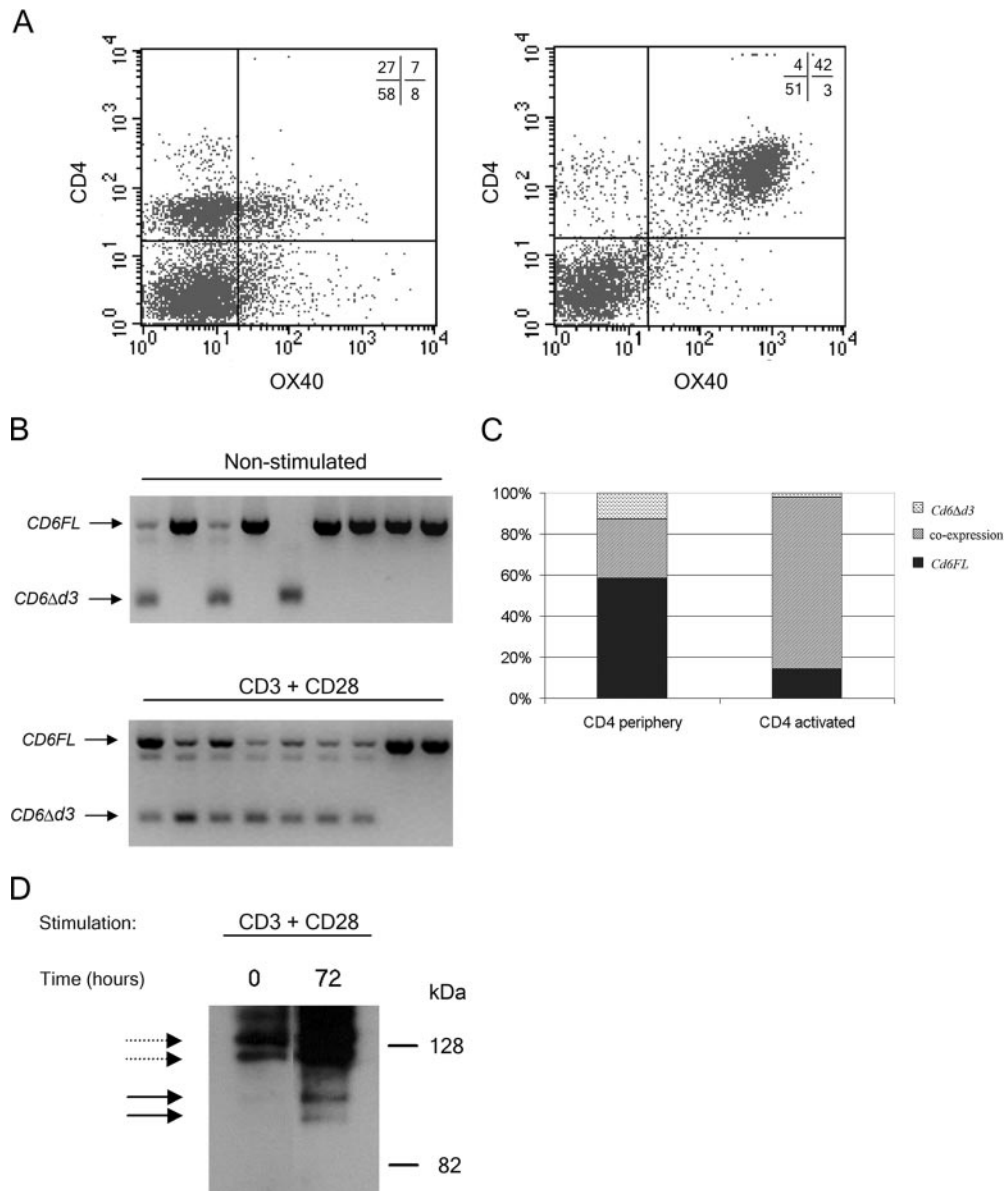


**FIGURE 5.** CD6Δd3 expression is up-regulated upon activation. *A*, Rat spleen cells were activated in vitro via TCRαβ and CD28 for 72 h or left untreated. OX40 expression was analyzed by flow cytometry in CD4<sup>+</sup>-resting cells (*left panel*) and at day 3 of activation (*right plot*). Individual CD4<sup>+</sup>OX40<sup>+</sup>-activated cells were sorted from the gated CD6<sup>high</sup> population (*upper right quadrant*). The percentage of cells in each quadrant is indicated in the *upper right*. *B*, RT-PCR performed on activated vs nonactivated individual cells sorted. Gel is only illustrative; over 40 cells were always considered for calculations. *C*, Percentage of activated CD4<sup>+</sup>OX40<sup>+</sup> T cells vs nonactivated T cells expressing CD6FL, CD6Δd3, or showing coexpression. *D*, Rat splenocytes were activated by TCRαβ and CD28 mAb for 72 h or left untreated. After that time, cells were collected, lysed, and immunoprecipitated with OX52. CD6 was detected by Western blotting. Dashed arrows indicate high molecular mass CD6 isoforms, presumably containing domain 3 of CD6, and thick arrows indicate low molecular mass isoforms, suggestive of CD6 isoforms lacking domain 3.

was immunoprecipitated and detected by immunoblotting. Interestingly, after 72 h of activation two smaller isoforms of 106 and 99 kDa were expressed (Fig. 5D, solid arrows). It is plausible that these new isoforms correspond to protein products missing domain 3.

#### *T cell activation controls expression of the human SRCR domain 3 of CD6*

We obtained from human PBMC, as well as from the Jurkat cell line E6.1 (data not shown), cDNAs coding for the full-length molecule and also several PCR products with sizes ranging from 2,000 down to 1,600 bp (Fig. 6A, *middle lane*). We then tested for the existence of the CD6Δd3 isoform in human cells, and following the same strategy as for the rat CD6 gene, per-

formed RT-PCR amplifying just the extracellular domain-coding sequences. A prominent band of 1,200 bp and also a 300 nt shorter product were clearly detected (Fig. 6A, *right lane*, compare with Fig. 4A).

Next, we gel-purified the cDNA fragments, subcloned them, and sequenced multiple clones. We could confirm that the message coding for the extracellular domain isoform CD6Δd3 (GenBank accession no. DQ786329), lacking exon 5, was present in both PBMC and E6.1 Jurkat cells. An additional mRNA species (GenBank accession no. DQ786330) was detected in the cells analyzed, lacking not only exon 5 but also exon 6, which codes for a linker between the membrane proximal SRCR domain and the transmembrane stretch (Fig. 6B).

The previous results suggested that, as in the rat, multiple CD6 isoforms coexist in human T cells. We compared the expression of



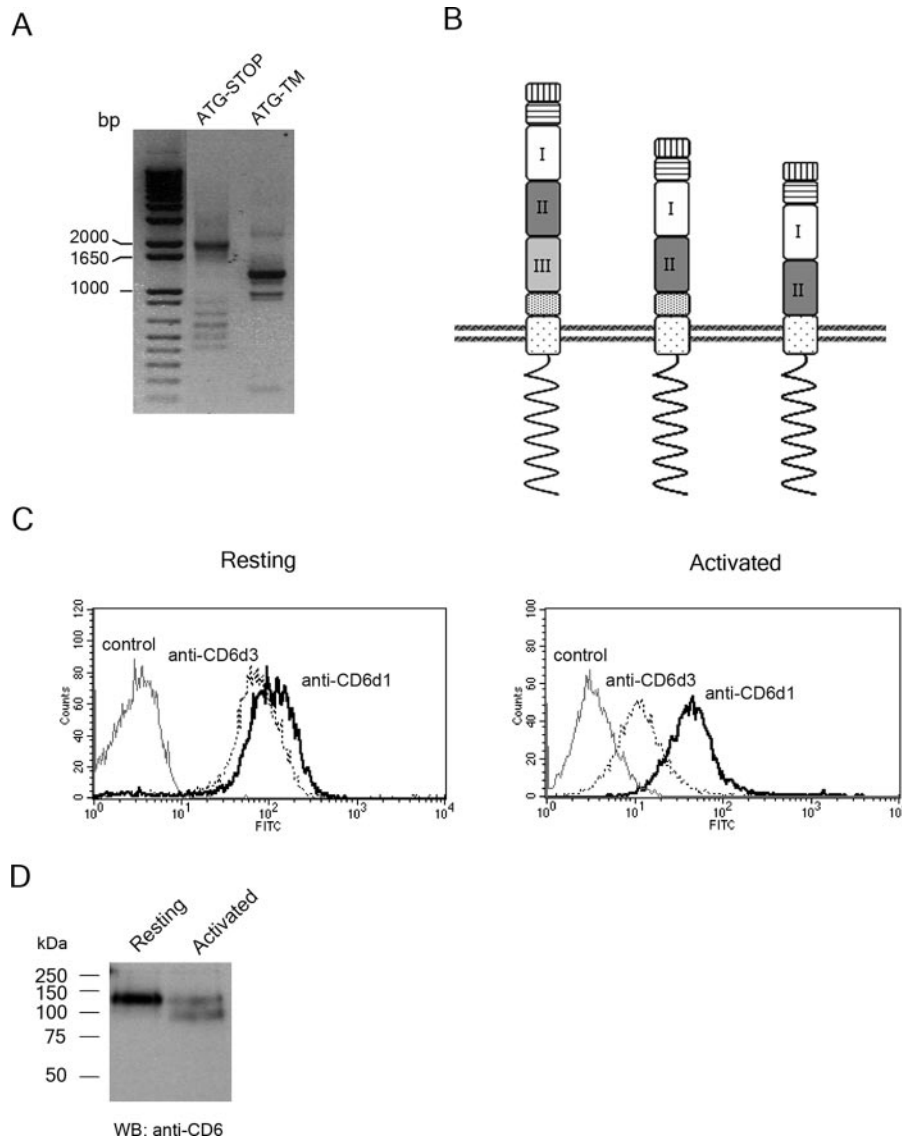
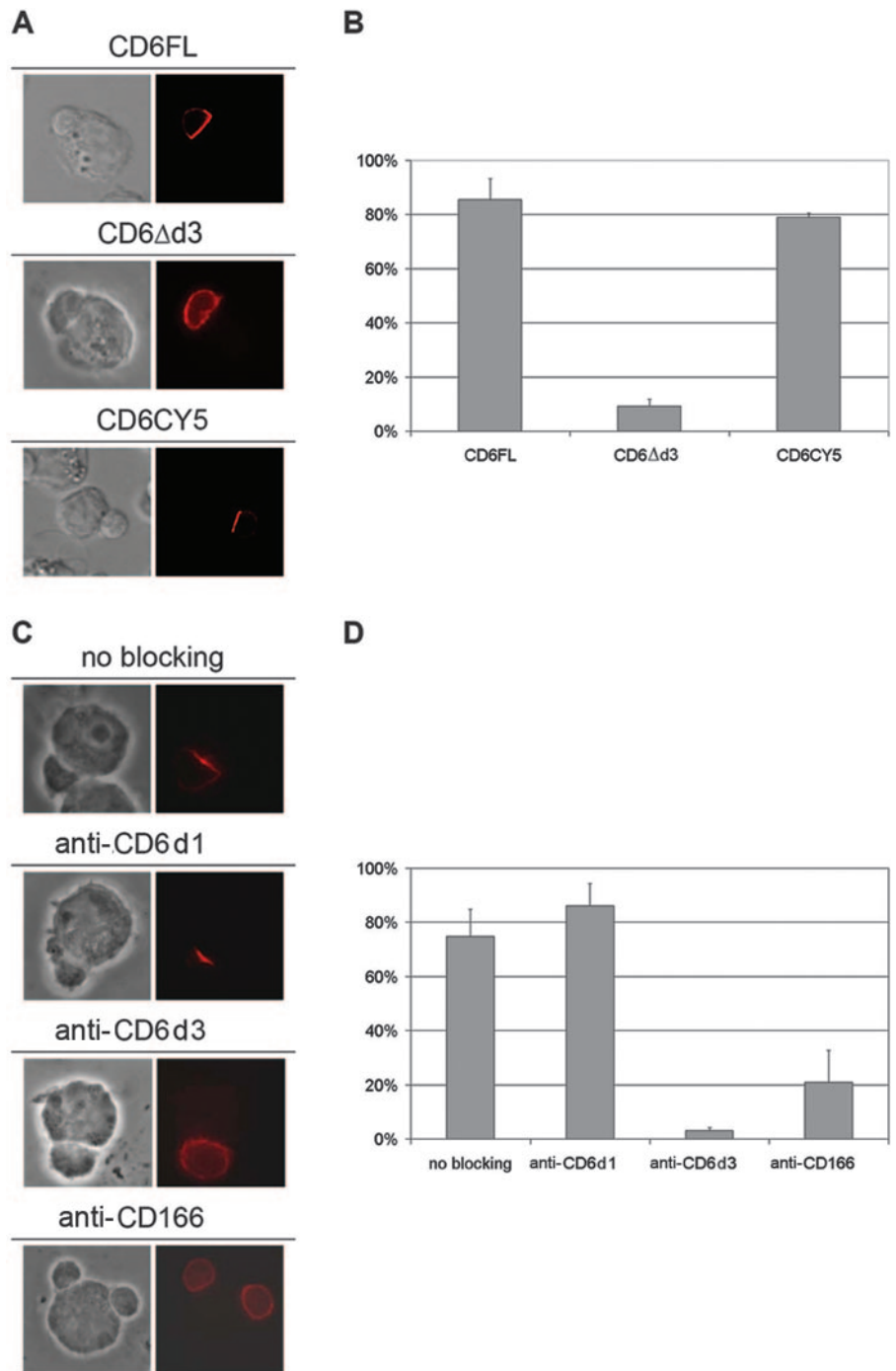


**FIGURE 6.** Increased expression of CD6 $\Delta$ d3 in human cells, upon activation. **A**, Total RNA from human PBMC was used for RT-PCR and amplified from the ATG up to the transmembrane region (TM) or the STOP codon. The cDNA products were analyzed on gels, isolated, and sequenced. The *middle lane* shows the amplification of the full-length cDNA, clearly visible at 2,071 bp, and additional shorter products between 2,000 and 1,600 bp. As can be seen on the *right lane*, products of amplification of the extracellular region were obtained, including the full-length isoform of 1,200 bp and a smaller band of 900 bp. **B**, Schematic representation of the extracellular isoforms of human CD6 protein deduced from sequencing of the RT-PCR products obtained from human PBMC and E6.1 Jurkat cells. The full-length transcript was the most abundant in both PBMC and Jurkat E6.1 cells. The CD6 $\Delta$ d3 isoform excluding only exon 5 and also a similar isoform excluding additionally exon 6 were also recurrent, as evaluated by the frequency in the number of clones sequenced. **C**, Human primary T cells isolated from peripheral blood, using the RosetteSep human T cell enrichment mixture, were analyzed by flow cytometry for the expression of CD6 extracellular isoforms by using specific Abs recognizing either domain 1, UMCD6, or domain 3, OX126. The expression is compared with the fluorescence of the control secondary Ab FITC conjugated (*left panel*). After 3 days of stimulation with PHA, a significant decrease in the level of expression of the isoform lacking domain 3 could be detected, as can be seen by using the same Abs (*right panel*). PHA-activated cells were gated based on the expression of the activation marker CD71 (data not shown). **D**, The expression of CD6 in resting cells, and in cells 3 days postactivation with PHA, was analyzed by Western blotting with anti-CD6 MEM-98 mAb. A decrease in the level of the higher molecular mass isoform and the appearance of a lower molecular mass species can be seen after activation.

the putative CD6 extracellular isoforms between resting and PHA-activated T cells. For detection of CD6, we used mAbs specific for CD6 domain 3, OX126, or CD6 domain 1, UMCD6 (22). In purified resting T lymphocytes, both SRCR domains 1 and 3 of CD6 are expressed at similar levels, a result consistent with resting T cells expressing mostly CD6FL (Fig. 6C, *left panel*). In contrast, 3 days following stimulation with PHA, the expression of domain 3 was significantly down-modulated, compared with the relatively unchanged labeling of domain 1 (Fig. 6C, *right panel*).

We have also analyzed the changes on CD6 isoform expression upon cell activation by immunoblotting. Nonactivated human T cells expressed a major CD6 species of 130 kDa. However, 3 days postactivation with PHA, an additional CD6 isoform with a molecular mass of 97 kDa was clearly detected by immunoblotting, whereas the expression of the larger CD6 species was decreased to a level equivalent to that of the smaller isoform (Fig. 6D). Together, the cytometry and Western blotting analysis suggest that, following activation of human T lymphocytes, the expression of

**FIGURE 7.** Human CD6 localizes at the synapse depending on the binding of the CD6 SRCR domain 3 to endogenous CD166 expressed at the surface of Raji cells. *A*, T cells expressing CD6FL-GFP, CD6 $\Delta$ d3-GFP, or CD6CY5-GFP (shown in red) were incubated with Raji B cells prepulsed with 1  $\mu$ g/ml superantigen mix and analyzed for localization at the IS. *B*, Bar chart representing CD6 accumulation at the IS in T cells expressing the different CD6 isoforms. Results are from three independent experiments. *C*, Ab-blocking interference of CD6-ligand interaction on the localization of CD6 at the IS. Before incubation with superantigen-pulsed Raji B cells, T lymphocytes were incubated with the mAbs UMCD6, recognizing CD6 domain 1 (anti-CD6d1), or OX126, recognizing CD6 domain 3 (anti-CD6d3), or left untreated. Alternatively, Raji B cells were treated with anti-CD166 mAb (anti-CD166). The localization of CD6 was performed by immunolabeling with UMCD6-FITC, or with RAM-FITC in the case of blocking with anti-CD6d3. *D*, Quantification of the number of cell conjugates displaying CD6 at the IS.



full-length CD6 is partially down-regulated with the concomitant appearance of the CD6 $\Delta$ d3 isoform.

#### Human CD6 targeting to the IS: analysis of binding to CD166

We proceeded to confirm that human CD6 isoforms behaved similarly to those analyzed in rat, regarding translocation to the IS upon Ag recognition. Human T lymphocytes were induced to express full-length human CD6 (CD6FL), the CD6 $\Delta$ d3 isoform, or the CD6CY5 mutant, all fused to GFP. Following incubation of T cells with superantigen-loaded Raji cells, which expressed endogenous CD166 at high levels on the surface (data not shown), conjugate formation and CD6 translocation to the synapse was evaluated in all conditions. Both CD6FL and CD6CY5 localized very efficiently to the IS in ~80% of total conjugates, whereas

CD6 $\Delta$ d3 was typically dispersed throughout the cell surface (Fig. 7, *A* and *B*).

To test whether nonengineered endogenous CD6 expressed in T lymphocytes was still capable of targeting to the synapse, and that this effect was due to the binding to endogenous Raji-expressed CD166, we evaluated, through immunofluorescence, the localization of CD6 in T:Raji interfaces using blocking, as well as non-blocking Abs. Characteristically, CD6 confined to the synapse in 75% of unblocked T cell:Raji conjugates, a figure that did not significantly change when T cells had been previously incubated with UMCD6, an Ab recognizing domain 1 of CD6, and not able to block CD6-CD166 interactions (Fig. 7, *C* and *D*). However, when T cells had been incubated with the blocking, anti-CD6 domain 3, mAb OX126, CD6 localization at the synapse dropped

dramatically to residual levels (Fig. 7, *C* and *D*). Similarly, previous incubation of Raji with the CD166 mAb, described to obstruct the interaction with CD6 (37), resulted in the noticeable reduction of the translocation of CD6 to the synapse (Fig. 7, *C* and *D*), in agreement with a previous study using blocking CD166 Abs in T cell-dendritic cell conjugates (15). Taken together, the results demonstrate that the direct interaction between CD166 and the SRCR domain 3 of CD6 is the driving force for the translocation of CD6 to the IS.

## Discussion

The great majority of mammalian genes yield multiple mRNA transcripts arising from diverse promoter selection, alternative splicing, and/or differential polyadenylation (43). Despite the frequency and potential impact of this phenomenon, particularly relevant in the immune system, the cases in which distinct functional properties have been assigned to different isoforms of the same molecule are scarce. In T lymphocytes, just a few examples of naturally occurring alternatively spliced-encoded isoforms of transmembrane proteins have been reported, and only in three cases with clear distinct functional consequences: CTLA4 and CD95 can become transmembrane molecules instead of being secreted (44, 45), as a consequence of the inclusion of membrane-spanning domains following cell stimulation; and CD45, upon T cell differentiation, is produced with a shorter N-terminal extracellular domain, which increases the dimerization capacity of the molecule (46). Alongside this general trend, multiple isoforms resulting from alternative splicing of cytoplasmic domain-coding exons have been described for CD6, but with no distinct functions assigned (18, 28–30). In this study, we describe a rare example of a functional consequence resulting from alternative splicing in molecules of the immune system: the localization of CD6 with respect to the IS depends on the regulated expression of the CD166 binding domain by means of alternative mRNA splicing.

Targeting of CD6 to the synapse can be driven by simple lateral diffusion and does not require cytoskeletal reorganization, because deletion of the cytoplasmic tail did not affect the ability of CD6 to localize to the synapse. Therefore, the positioning of CD6 within the synapse must be largely determined by molecular interactions established with the contacting cell. Both human and rat CD6 molecules targeted very efficiently to the IS when expressing the CD166 binding domain, provided that the APCs were equally expressing CD166. However, when using T cells expressing CD6 $\Delta$ d3, synaptic localization of that isoform could still be attained in a small percentage of conjugates. A putative role for domain 2 of CD6, now substituting the positioning of domain 3 in CD6 $\Delta$ d3, or even for the membrane-juxtaposed stalk region, could be considered, given the fact that previous studies had suggested a minor participation of these domains in the binding to CD166 (22, 23). Nevertheless, it is the presence of domain 3 that largely determines CD6 synaptic localization, and thus regulation of its expression is the key event establishing the positioning of CD6 upon conjugate formation and T cell activation.

The mode of action of CD6 appears to be significantly different from that of other accessory molecules that influence signaling at or near the IS. CD2 binding to its ligand CD58 (CD48 in rodents) contributes to enhanced signaling, because it associates with intracellular-positive mediators (47). CD28 and CTLA-4 have devised a scheme whereby sequential expression of each molecule, combined with binding to one of the alternative ligands, CD80 and CD86 (themselves also sequentially expressed during T cell-APC interactions), drives responses from costimulation to inhibition (48). Differences in the affinity and avidity of binding determine

the selective recruitment of CD28 or CTLA-4 to the IS upon recognition of CD86 or CD80 (49).

Meanwhile CD6, which was reported to deliver costimulatory signals as strongly as CD28 (15), mimics CD28 distribution with respect to synaptic localization, in that it is recruited to the IS at the onset of activation, and, according to the present study, is excluded from the cellular interface at later stages. However, it may display this same pattern of localization through a completely different mechanism: expressing the SRCR domain 3, CD6 is directed to the synapse where it can control signaling; choosing not to express the SRCR domain 3, it is no longer restricted to the cellular interface and its regulatory function may be diluted.

The reason why CD6 does not simply switch off its expression is not immediately evident. However, the existence of an alternative ligand for CD6 raises new perspectives for its overall function (50). If the new ligand can interact with a different part of CD6, switching from full-length to  $\Delta$ d3 may allow CD6 to shift from the synapse established with the APC to either an interaction with a second adjacent cell or again to the initial interface, provided that the second ligand is present. Differential molecular interactions could then modulate the behavior of CD6.

The apparent steadiness in expression of the alternative CD6 mRNAs in different mature subpopulations may suggest that CD6 $\Delta$ d3 can define small subsets of thymocytes and mature T cells; however, the switch to the expression of the shorter isoform observed upon stimulation of T cells is undoubtedly a consequence or a product of activation. In the resting state, the majority of the cells express mainly the full-length CD6 form; upon productive T cell stimulation, there is a partial substitution of the full-length isoform by a substantial number of CD6 molecules per cell that no longer express the CD166 binding domain and thus are not restricted to the IS. This type of regulation of splicing is not unique, because it has long been known to control the expression of CD45 isoforms (51, 52). The novel CD6 isoform reported in this study seems to have a more obvious function because it disables the interaction of the protein with its ligand. Productive TCR recognition of Ag may signal for the shorter CD6 isoform to be produced, and this response may reduce the activity of CD6 at the synapse, possibly inducing a different behavior.

The expression of the CD6FL isoform seems to be highly favored in the DP stage in the thymus. Previous observations suggest that CD6 can be involved in positive selection, where it correlates with the expression of CD69 in DP thymocytes (53). Moreover, an inverse correlation between thymocyte CD6 expression and the rate of apoptosis has been demonstrated. Our results may be indicative of a mechanism of regulation where the expression of CD6FL capable of interacting with the ligand CD166, expressed by thymic epithelial cells, is favored at the DP stage and bypassed later on during thymic selection.

## Acknowledgments

We thank Simon Davis (Weatherall Institute of Molecular Medicine, University of Oxford, U.K.) and Neil Barclay (Sir William Dunn School of Pathology, University of Oxford, U.K.) for helpful discussions and critical reading of the manuscript.

## Disclosures

The authors have no financial conflict of interest.

## References

1. Shaw, A. S., and M. L. Dustin. 1997. Making the T cell receptor go the distance: a topological view of T cell activation. *Immunity* 6: 361–369.
2. Monks, C. R., B. A. Freiberg, H. Kupfer, N. Sciaky, and A. Kupfer. 1998. Three-dimensional segregation of supramolecular activation clusters in T cells. *Nature* 395: 82–86.

3. Grakoui, A., S. K. Bromley, C. Sumen, M. M. Davis, A. S. Shaw, P. M. Allen, and M. L. Dustin. 1999. The immunological synapse: a molecular machine controlling T cell activation. *Science* 285: 221–227.
4. Bromley, S. K., W. R. Burack, K. G. Johnson, K. Somersalo, T. N. Sims, C. Sumen, M. M. Davis, A. S. Shaw, P. M. Allen, and M. L. Dustin. 2001. The immunological synapse. *Annu. Rev. Immunol.* 19: 375–396.
5. Bromley, S. K., A. Iaboni, S. J. Davis, A. Whitty, J. M. Green, A. S. Shaw, A. Weiss, and M. L. Dustin. 2001. The immunological synapse and CD28-CD80 interactions. *Nat. Immunol.* 2: 1159–1166.
6. Davis, S. J., and P. A. van der Merwe. 1996. The structure and ligand interactions of CD2: implications for T-cell function. *Immunol. Today* 17: 177–187.
7. Aruffo, A., M. B. Melnick, P. S. Linsley, and B. Seed. 1991. The lymphocyte glycoprotein CD6 contains a repeated domain structure characteristic of a new family of cell surface and secreted proteins. *J. Exp. Med.* 174: 949–952.
8. Gangemi, R. M., J. A. Swack, D. M. Gaviria, and P. L. Romain. 1989. Anti-T12, an anti-CD6 monoclonal antibody, can activate human T lymphocytes. *J. Immunol.* 143: 2439–2447.
9. Bott, C. M., J. B. Doshi, C. Morimoto, P. L. Romain, and D. A. Fox. 1993. Activation of human T cells through CD6: functional effects of a novel anti-CD6 monoclonal antibody and definition of four epitopes of the CD6 glycoprotein. *Int. Immunol.* 5: 783–792.
10. Osorio, L. M., C. A. Garcia, M. Jondal, and S. C. Chow. 1994. The anti-CD6 mAb, IOR-T1, defined a new epitope on the human CD6 molecule that induces greater responsiveness in T cell receptor/CD3-mediated T cell proliferation. *Cell. Immunol.* 154: 123–133.
11. Rasmussen, R. A., S. L. Counts, J. F. Daley, and S. F. Schlossman. 1994. Isolation and characterization of CD6- T cells from peripheral blood. *J. Immunol.* 152: 527–536.
12. Patel, D. D., S. F. Wee, L. P. Whichard, M. A. Bowen, J. M. Pesando, A. Aruffo, and B. F. Haynes. 1995. Identification and characterization of a 100-kD ligand for CD6 on human thymic epithelial cells. *J. Exp. Med.* 181: 1563–1568.
13. Gimferrer, I., M. Calvo, M. Mittelbrunn, M. Farnós, M. R. Sarrias, C. Enrich, J. Vives, F. Sánchez-Madrid, and F. Lozano. 2004. Relevance of CD6-mediated interactions in T cell activation and proliferation. *J. Immunol.* 173: 2262–2270.
14. Hassan, N. J., A. N. Barclay, and M. H. Brown. 2004. Optimal T cell activation requires the engagement of CD6 and CD166. *Eur. J. Immunol.* 34: 930–940.
15. Zimmerman, A. W., B. Joosten, R. Torensma, J. R. Parnes, F. N. van Leeuwen, and C. G. Figdor. 2006. Long-term engagement of CD6 and ALCAM is essential for T cell proliferation induced by dendritic cells. *Blood* 107: 3212–3220.
16. Wee, S., G. L. Schieven, J. M. Kirihara, T. T. Tsu, J. A. Ledbetter, and A. Aruffo. 1993. Tyrosine phosphorylation of CD6 by stimulation of CD3: augmentation by the CD4 and CD2 coreceptors. *J. Exp. Med.* 177: 219–223.
17. Hassan, N. J., S. J. Simmonds, N. G. Clarkson, S. Hanrahan, M. J. Puklavec, M. Bomb, A. N. Barclay, and M. H. Brown. 2006. CD6 regulates T-cell responses through activation-dependent recruitment of the positive regulator SLP-76. *Mol. Cell. Biol.* 26: 6727–6738.
18. Robinson, W. H., H. E. Neuman de Vegvar, S. S. Prohaska, J. W. Rhee, and J. R. Parnes. 1995. Human CD6 possesses a large, alternatively spliced cytoplasmic domain. *Eur. J. Immunol.* 25: 2765–2769.
19. Castro, M. A. A., R. J. Nunes, M. I. Oliveira, P. A. Tavares, C. Simões, J. R. Parnes, A. Moreira, and A. M. Carmo. 2003. OX52 is the rat homologue of CD6: evidence for an effector function in the regulation of CD5 phosphorylation. *J. Leukocyte Biol.* 73: 183–190.
20. Gimferrer, I., M. Farnos, M. Calvo, M. Mittelbrunn, C. Enrich, F. Sanchez-Madrid, J. Vives, and F. Lozano. 2003. The accessory molecules CD5 and CD6 associate on the membrane of lymphoid T cells. *J. Biol. Chem.* 278: 8564–8571.
21. Aruffo, A., M. A. Bowen, D. D. Patel, B. F. Haynes, G. C. Starling, J. A. Gebe, and J. Bajorath. 1997. CD6-ligand interactions: a paradigm for SRCR domain function? *Immunol. Today* 18: 498–504.
22. Bowen, M. A., J. Bajorath, A. W. Siadak, B. Modrell, A. R. Malacko, H. Marquardt, S. G. Nadler, and A. Aruffo. 1996. The amino-terminal immunoglobulin-like domain of activated leukocyte cell adhesion molecule binds specifically to the membrane-proximal scavenger receptor cysteine-rich domain of CD6 with a 1:1 stoichiometry. *J. Biol. Chem.* 271: 17390–17396.
23. Whitney, G. S., G. C. Starling, M. A. Bowen, B. Modrell, A. W. Siadak, and A. Aruffo. 1995. The membrane-proximal scavenger receptor cysteine-rich domain of CD6 contains the activated leukocyte cell adhesion molecule binding site. *J. Biol. Chem.* 270: 18187–18190.
24. Hohenester, E., T. Sasaki, and R. Timpl. 1999. Crystal structure of a scavenger receptor cysteine-rich domain sheds light on an ancient superfamily. *Nat. Struct. Biol.* 6: 228–232.
25. Davis, S. J., S. Ikemizu, E. J. Evans, L. Fugger, T. R. Bakker, and P. A. van der Merwe. 2003. The nature of molecular recognition by T cells. *Nat. Immunol.* 4: 217–224.
26. Dustin, M. L., D. E. Golan, D.-M. Zhu, J. M. Miller, W. Meier, E. A. Davies, and P. A. van der Merwe. 1997. Low affinity interaction of human or rat T cell adhesion molecule CD2 with its ligand aligns adhering membranes to achieve high physiological affinity. *J. Biol. Chem.* 272: 30889–30898.
27. Evans, E. J., M. A. A. Castro, R. O'Brien, A. Kearney, H. Walsh, L. M. Sparks, M. G. Tucknott, E. A. Davies, A. M. Carmo, P. A. van der Merwe, et al. 2006. Crystal structure and binding properties of the CD2 and CD244 (2B4)-binding protein, CD48. *J. Biol. Chem.* 281: 29309–29320.
28. Robinson, W. H., S. S. Prohaska, J. C. Santoro, H. L. Robinson, and J. R. Parnes. 1995. Identification of a mouse protein homologous to the human CD6 T cell surface protein and sequence of the corresponding cDNA. *J. Immunol.* 155: 4739–4748.
29. Whitney, G., M. Bowen, M. Neubauer, and A. Aruffo. 1995. Cloning and characterization of murine CD6. *Mol. Immunol.* 32: 89–92.
30. Bowen, M. A., G. S. Whitney, M. Neubauer, G. C. Starling, D. Palmer, J. Zhang, N. J. Nowak, T. B. Shows, and A. Aruffo. 1997. Structure and chromosomal location of the human CD6 gene: detection of five human CD6 isoforms. *J. Immunol.* 158: 1149–1156.
31. Gluzman, T. 1981. SV40-transformed simian cells support the replication of early SV40 mutants. *Cell* 23: 175–182.
32. Epstein, M. A., B. G. Achong, Y. M. Barr, B. Zajac, G. Henle, and W. Henle. 1966. Morphological and virological investigations on cultured Burkitt tumor lymphoblasts (strain Raji). *J. Natl. Cancer Inst.* 37: 547–559.
33. Robinson, A. P., M. Puklavec, and D. W. Mason. 1986. MRC OX-52: a rat T-cell antigen. *Immunology* 57: 527–531.
34. Hüning, T., H. J. Wallny, J. K. Hartley, A. Lawetzky, and G. Tiefenthaler. 1989. A monoclonal antibody to a constant determinant of the rat T cell antigen receptor that induces T cell activation: differential reactivity with subsets of immature and mature T lymphocytes. *J. Exp. Med.* 169: 73–86.
35. Tacke, M., G. J. Clark, M. J. Dallman, and T. Hüning. 1995. Cellular distribution and costimulatory function of rat CD28: regulated expression during thymocyte maturation and induction of cyclosporin A sensitivity of costimulated T cell responses by phorbol ester. *J. Immunol.* 154: 5121–5127.
36. Bazil, V., I. Stefanova, I. Hilgert, H. Kristofova, S. Vanek, A. Bukovsky, and V. Horejsi. 1989. Monoclonal antibodies against human leucocyte antigens, III: antibodies against CD45R, CD6, CD44 and two newly described broadly expressed glycoproteins MEM-53 and MEM-102. *Folia Biol.* 35: 289–297.
37. Kishimoto, T., A. E. G. von dem Borne, S. M. Goyert, D. Y. Mason, M. Miyasake, L. Moretta, K. Okumura, S. Shaw, T. A. Springer, K. Sagamura, and H. Zola. 1997. *Leukocyte Typing VI: White Cell Differentiation Antigens*. Garland Publishing, London.
38. Mizushima, S., and S. Nagata. 1990. pEF-BOS, a powerful mammalian expression vector. *Nucleic Acids Res.* 18: 5322.
39. Castro, M. A. A., P. A. Tavares, M. S. Almeida, R. J. Nunes, M. D. Wright, D. Mason, A. Moreira, and A. M. Carmo. 2002. CD2 physically associates with CD5 in rat T lymphocytes with the involvement of both extracellular and intracellular domains. *Eur. J. Immunol.* 32: 1509–1518.
40. Carmo, A. M., M. A. A. Castro, and F. A. Arosa. 1999. CD2 and CD3 associate independently with CD5 and differentially regulate signaling through CD5 in Jurkat T cells. *J. Immunol.* 163: 4238–4245.
41. Peixoto, A., M. Monteiro, B. Rocha, and H. Veiga-Fernandes. 2004. Quantification of multiple gene expression in individual cells. *Genome Res.* 14: 1938–1947.
42. Paterson, D. J., W. A. Jefferies, J. R. Green, M. R. Brandon, P. Corthesy, M. Puklavec, and A. F. Williams. 1987. Antigens of activated rat T lymphocytes including a molecule of 50,000 Mr detected only on CD4 positive T blasts. *Mol. Immunol.* 24: 1281–1290.
43. Johnson, J. M., J. Castle, P. Garrett-Engele, Z. Kan, P. M. Loerch, C. D. Armour, R. Santos, E. E. Schadt, R. Stoughton, and D. D. Shoemaker. 2003. Genome-wide survey of human alternative pre-mRNA splicing with exon junction microarrays. *Science* 302: 2141–2144.
44. Cheng, J., T. Zhou, C. Liu, J. P. Shapiro, M. J. Brauer, M. C. Kiefer, P. J. Barr, and J. D. Mountz. 1994. Protection from Fas-mediated apoptosis by a soluble form of the Fas molecule. *Science* 263: 1759–1762.
45. Magistrelli, G., P. Jeannin, N. Herbault, A. Benoit De Coignac, J. F. Gauchat, J. Y. Bonnefoy, and Y. Delneste. 1999. A soluble form of CTLA-4 generated by alternative splicing is expressed by nonstimulated human T cells. *Eur. J. Immunol.* 29: 3596–3602.
46. Xu, Z., and A. Weiss. 2002. Negative regulation of CD45 by differential homodimerization of the alternatively spliced isoforms. *Nat. Immunol.* 3: 764–771.
47. Carmo, A. M., D. W. Mason, and A. D. Beyers. 1993. Physical association of the cytoplasmic domain of CD2 with the tyrosine kinases p56<sup>lck</sup> and p59<sup>lyn</sup>. *Eur. J. Immunol.* 23: 2196–2201.
48. van der Merwe, P. A., and S. J. Davis. 2003. Molecular interactions mediating T cell antigen recognitions. *Annu. Rev. Immunol.* 21: 659–684.
49. Pentcheva-Hoang, T., J. G. Egen, K. Wojnoonski, and J. P. Allison. 2004. B7-1 and B7-2 selectively recruit CTLA-4 and CD28 to the immunological synapse. *Immunity* 21: 401–413.
50. Saifullah, M. K., D. A. Fox, S. Sarkar, S. M. A. Abidi, J. Endres, J. Piktet, T. M. Haqqi, and N. G. Singer. 2004. Expression and characterization of a novel CD6 ligand in cells derived from joint and epithelial tissues. *J. Immunol.* 173: 6125–6133.
51. Ralph, S. J., M. L. Thomas, C. C. Morton, and I. S. Trowbridge. 1987. Structural variants of human T200 glycoprotein (leukocyte-common antigen). *EMBO J.* 6: 1251–1257.
52. Streuli, M., L. R. Hall, Y. Saga, S. F. Schlossman, and H. Saito. 1987. Differential usage of three exons generates at least five different mRNAs encoding human leukocyte common antigens. *J. Exp. Med.* 166: 1548–1566.
53. Singer, N. G., D. A. Fox, T. M. Haqqi, L. Beretta, J. S. Endres, S. Prohaska, J. R. Parnes, J. Bromberg, and R. M. Sramkoski. 2002. CD6: expression during development, apoptosis and selection of human and mouse thymocytes. *Int. Immunol.* 14: 585–597.
54. Bowen, M. A., A. A. Aruffo, and J. Bajorath. 2000. Cell surface receptors and their ligands: in vitro analysis of CD6-CD166 interactions. *Proteins* 40: 420–428.